Bol. Soc. Paran. Mat.
©SPM – E-ISSN-2175-1188
SPM: www.spm.uem.br/bspm

(3s.) **v. 2025 (43)** : 1–13.
ISSN-0037-8712
doi:10.5269/bspm.77128

Mathematical Analysis of Thermal Management in Photovoltaic Modules

A. KADYRI*, EM. ASSAID, K. KANDOUSSI and O. SOUHAR

ABSTRACT: Thermal management is a key factor in optimizing the performance and longevity of photovoltaic (PV) systems. This work presents a two-dimensional thermal model based on fully explicit finite difference methods to simulate heat transfer across the layered structure of PV modules. The model incorporates conduction, convection, and radiation, along with realistic boundary conditions and material properties. Validation against experimental data under varying irradiance confirms its strong predictive capabilities. Multiple statistical indicators demonstrate high accuracy and consistency between modeled and observed temperatures. The results highlight critical thermal gradients and potential hotspots that affect PV efficiency. This modeling framework offers valuable insights for improving panel design and implementing efficient thermal control strategies. It also contributes to the theoretical understanding of heat transfer in PV systems, supporting future advancements in high-efficiency, climate-resilient solar technologies.

Key Words: *2D finite difference, Heat transfer modes, PV cell, PV module, Simulation model, Statistical indices, Validation model.*

Contents

1 Introduction **1**

2 Simplified 2D Heat Transfer Equation Model **3**
2.1 Modes of Heat Transfer . . . 3
2.2 Problem description . . . 4
2.3 Internal Heat Generations . . . 5
2.4 Boundary Conditions . . . 6

3 Numerical solution **7**
3.1 Fully-explicit Finite Difference Methods . . . 7
3.1.1 Statistical indices . . . 7
3.2 Results presentation . . . 8
3.3 Model validation . . . 10
3.3.1 Comparison between modeled and observed data . . . 10

4 Discussion **11**

5 Conclusion and Perspectives **11**

1. Introduction

As the global shift towards sustainable energy solutions gains momentum, photovoltaic (PV) technology has emerged as a pivotal component in the transition to a greener future. The process of converting sunlight into electrical energy through PV panels is not only central to harnessing renewable resources but also presents significant engineering challenges, particularly in the realm of thermal management. The direct correlation between a panel's thermal characteristics and its operational efficiency necessitates a comprehensive exploration of the thermal dynamics within these systems.

The journey of photovoltaic technology from a specialized scientific interest to a primary energy source is marked by substantial advancements in materials science, electrical engineering, and thermal physics. Despite notable improvements in solar panel efficiency over time, performance remains hindered by thermal-induced limitations [19,11]. It is well-documented that the efficiency of PV cells can decrease

* Corresponding author

Submitted May 31, 2025. Published July 11, 2025
2010 *Mathematics Subject Classification:* 35B40, 35L70.

Typeset by $\mathcal{B}^{S}\mathcal{P}_{\mathcal{M}}$ style.
© Soc. Paran. de Mat.

by approximately 0.3% to 0.5% for each degree Celsius increase in temperature, highlighting the critical impact of thermal management on panel performance [1,5,6,7,10,18].

Unlike conventional 1D models [2], which only resolve temperature variations through the panel thickness, our 2D framework captures both thickness- and width-wise gradients. This provides a more accurate depiction of the thermal field while maintaining a significantly lower computational cost compared to full 3D finite element models [15].

The heat transfer mechanism within a solar panel is a complex interplay of thermal conduction, further complicated by the panel's multi-layered structure (Figure 1). Each layer, from the protective glass to the Tedlar backing, has distinct thermal and optical properties, contributing differently to the panel's overall thermal behavior. The generated heat in the photovoltaic cells must be efficiently dissipated to prevent adverse effects on power output and long-term reliability [10,13,21,23].

Addressing these complexities, we use Fully-Explicit Finite Difference Methods (FE-FDM) to model the two-dimensional (thickness-width) temperature distribution in the PV panel comprised of five layers: Glass, upper EVA, PV cells, lower EVA, and Tedlar. The detailed thermophysical properties of each layer, including thickness, thermal conductivity, density, and specific heat capacity, are summarized in Table 1 and serve as essential parameters for the numerical model.

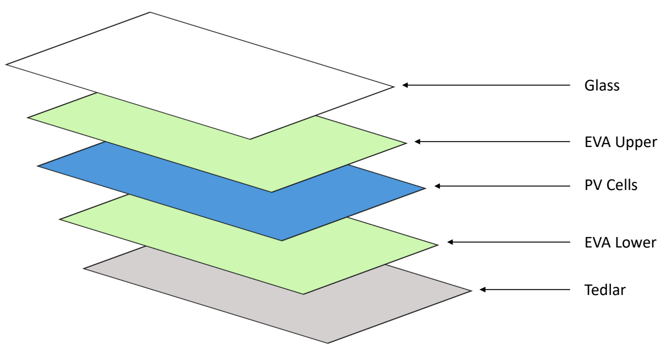

Figure 1: Solar panel layers

Using MATLAB for FE-FDM implementation, we aim to provide a detailed representation of the temperature gradients across these layers [25,26]. The governing heat transfer equation in our analysis with specific boundary conditions presented in [2,16,17,21] is:

$$\rho c_p \frac{\partial T}{\partial t} = \nabla \cdot (k \nabla T) + Q \tag{1.1}$$

where $\nabla\cdot(k\nabla T)$ signifies conductive heat transfer, k is the thermal conductivity, T represents temperature, t is time, Q denotes internal heat generation, ρ is material density, and c_p is specific heat capacity.

This research extends beyond the application of FDM to investigate the intricate thermal interactions within the panel's structure. By analyzing a standard five-layered setup, we aim to shed light on the nuanced heat transfer processes and their impact on panel performance. Our analysis not only identifies temperature profiles but also potential thermal bottlenecks that could impair the panel's efficiency and longevity.

Moreover, the empirical aspect of our study involves measuring temperature distributions on actual PV panels under varying environmental conditions, providing crucial validation for our theoretical models using statistical indices [8,11]. This comprehensive approach, bridging theoretical predictions with practical observations, offers profound insights into the thermal management of photovoltaic systems, setting the stage for innovations in panel design and operational strategies.

Through this work, we contribute to the expanding domain of photovoltaic research, offering a detailed understanding of thermal effects that can influence future developments in solar energy technology. Our findings not only augment our knowledge of photovoltaic thermal dynamics but also emphasize the importance of integrated thermal management strategies in optimizing the performance and durability of solar panels. The validation of our approach through empirical data reinforces the reliability of our model, making it a valuable tool for future research and development in the field of photovoltaic technology.

2. Simplified 2D Heat Transfer Equation Model

2.1. Modes of Heat Transfer

Heat transfer in a photovoltaic panels occurs primarily through three modes: conduction, convection, and radiation presented in figure 2. Each of these modes plays a crucial role in the thermal management of the panel and affects its overall efficiency.

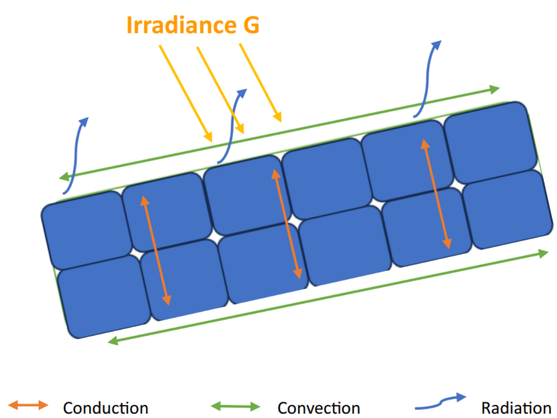

Figure 2: Typical heat transfer modes in photovoltaic panel

Conduction:

Conduction is the process of heat transfer through a solid material without the movement of the material itself. In a PV panel, conduction occurs through the different layers of the panel, such as the protective glass, EVA, PV cells, and Tedlar. Each layer has distinct thermal properties (thermal conductivity, density, specific heat capacity) that influence how heat is transferred through the panel. The heat conduction equation is given by:

$$\rho c_p \frac{\partial T}{\partial t} = \nabla \cdot (k \nabla T) + Q \tag{2.1}$$

where k is the thermal conductivity, ρ is the material density, c_p is the specific heat capacity, T is the temperature, and Q is the internal heat generation.

Convection:

Convection is the heat transfer between a solid surface and a moving fluid (such as air). In a PV panel, convection primarily occurs at the surface of the panel exposed to ambient air. The convection coefficient h depends on environmental conditions such as wind speed and air temperature. The convection condition is expressed by:

$$q_{conv} = h(T - T_{air}) \tag{2.2}$$

where T is the temperature of the panel surface and T_{air} is the ambient air temperature.

Radiation:

Radiation is the heat transfer through the emission of electromagnetic radiation. All bodies above absolute zero emit radiant energy. In a PV panel, radiation primarily occurs between the panel surface and the sky. The radiation condition is given by:

$$q_{rad} = \epsilon\sigma(T^4 - T_{sky}^4) \tag{2.3}$$

where ϵ is the emissivity of the surface, σ is the Stefan-Boltzmann constant, T is the temperature of the panel surface, and T_{sky} is the effective sky temperature.

2.2. Problem description

According the figure 3, the temperature T of the domain $\Omega = \bigcup_{i=1}^{5} \Omega_i$ is the solution of the heat transfer equation [4,21,24]:

$$\rho_i c_{p_i} \frac{\partial T}{\partial t} = \nabla(k_i \nabla T) + Q_i \quad for \quad i = 1, 2, ..., 5 \tag{2.4}$$

where:

- t is the time.
- T is the temperature.
- k is is the thermal conductivity.
- ρ is the mass density.
- c_p is the specific heat capacity.
- ∇^2 is the Laplacian operator in three dimensions, given by $\nabla^2 T = \frac{\partial^2 T}{\partial x^2} + \frac{\partial^2 T}{\partial y^2}$.
- Q is the heat source.

We assume that $0 \leq x \leq \sum_{i=1}^{5} e_i$ and $0 \leq y \leq h_{PV}$.

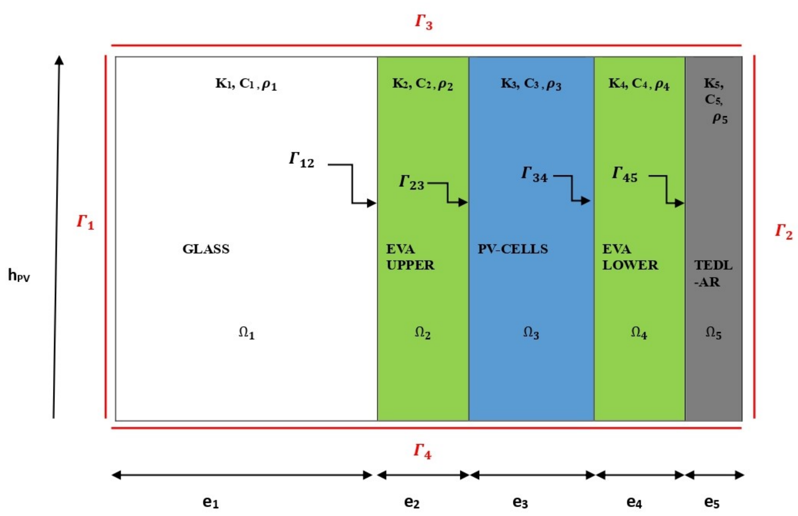

Figure 3: Geometry of the solar panel, $\Omega = \bigcup_{i=1}^{5} \Omega_i$ with $\partial\Omega = \bigcup_{i=1}^{4} \Gamma_i$

The temperature variation through the thickness of a PV solar panel is influenced by several factors such as the type of panel, atmospheric conditions, and the panel's thermal properties [2,3,11]

Table 1: Photovoltaic layer properties [2,3,11]

Layer	Thickness (m)	Conductivity k (W/m.K)	Density ρ (kg/m^3)	Heat Capacity c (J/kg.K)
Glass	0.002	1.8	3000	500
EVA	450×10^{-6}	0.35	960	2090
PV Cells	825×10^{-6}	148	2330	677
Tedlar	0.001	0.2	1200	1250

2.3. Internal Heat Generations

The internal heat generation within a Photovoltaic (PV) panel arises from the absorption of solar radiation across all its layers. When the layers of the PV panel, including the protective glass, EVA, PV cells, and Tedlar, absorb solar radiation, they convert a portion of this energy into heat. This process is a significant factor contributing to the warming of the PV panel during operation.

The solar irradiance G that is not converted into electricity accumulates as internal heat within each layer of the PV panel. The heat generation within each layer can be expressed as follows:

$$Q_i = \frac{\alpha_i \times G \times A}{V_i} \tag{2.5}$$

Where:

- α_i is the absorptivity of the i-th layer (specific to each layer, e.g., glass, EVA, PV cells, Tedlar).
- G is the solar irradiance.
- A is the area of the PV panel.
- V_i is the volume of the i-th layer.

In the case of PV cells, the internal heat generation is further influenced by the electrical efficiency η_{PV}, with the heat generation expressed as:

$$Q_{PV} = \frac{(1 - \eta_{PV}) \times \alpha_{PV} \times G \times A}{V_{PV}} \tag{2.6}$$

where the electrical efficiency η_{PV} is temperature-dependent and defined by:

$$\eta_{PV} = \eta_{PV,\text{ref}} \left[1 - \beta_{\text{ref}} \left(T_{PV,\text{cells}} - T_{\text{ref}}\right)\right] \tag{2.7}$$

Here, η_{PV} represents the electrical efficiency of the PV cells at a given temperature, $\eta_{PV,\text{ref}}$ is the reference electrical efficiency of the PV cells (0.15), β_{ref} is the temperature coefficient of the electrical efficiency (0.0045 C^{-1}), $T_{PV,\text{cells}}$ is the current temperature of the PV cells, and T_{ref} is the reference temperature (25°C).

In the heat generation equation, α_{PV} is the absorptivity of the PV cells, G is the solar irradiance, A is the cumulative front area of the PV cells, and V_{PV} is the total volume of the PV cells.

These equations account for the heat generated within each layer due to the non-converted solar irradiance. The absorptivity (α_i) specific to each layer and the efficiency (η_{PV}) of the PV cells are crucial factors in determining the amount of internal heat generated.

Efficient thermal management strategies are essential to handle this internal heat generation and maintain the optimal operating temperature of the PV panel. Effective heat dissipation mechanisms can help prevent overheating, thereby enhancing the overall performance and longevity of the PV panels.

2.4. Boundary Conditions

To solve this equation, it is essential to set suitable and reasonable boundary conditions [3,4].

- On Γ_1 ($0 \leq y \leq h_{PV}$ and $x = 0$):

We can combine the radiation and convection conditions to get a more comprehensive representation of heat transfer at the surface of an object like a solar panel. In fact, in many practical scenarios, this is the real situation.
The combination of the two gives:

$$q_{tot} = q_{conv} + q_{rad} = h(T - T_{air}) + \epsilon\sigma(T^4 - T_{sky}^4) \tag{2.8}$$

where h is the convection coefficient, T_{air} is the ambient air temperature, ϵ is the emissivity of the surface, σ is the Stefan-Boltzmann constant, and T_{sky} is the effective sky temperature.
With the sky temperature defined in [22] by:

$$T_{sky} = 0.0552 \times (T_{air})^{\frac{3}{2}} \tag{2.9}$$

Then, the combined boundary condition at Γ_1 is thus:

$$-k_1 \frac{\partial T}{\partial n} = h(T - T_{air}) + \epsilon\sigma(T^4 - T_{sky}^4) \tag{2.10}$$

This equation accounts for both heat loss by convection to the ambient air and radiation between the panel surface and the sky. It's a realistic representation of heat transfer mechanisms at the surface of solar panels or any other object exposed to the open air.

- On Γ_2 ($0 \leq y \leq h_{PV}$ and $x = \sum_{i=1}^{5} e_i$):

This is the base of the panel, where a convection-type condition is also appropriate.

$$-k_5 \frac{\partial T}{\partial n} = h(T - T_{air}) \tag{2.11}$$

- On Γ_3 ($0 \leq x \leq \sum_{i=1}^{5} e_i$ and $y = h_{PV}$) and on Γ_4 ($0 \leq x \leq \sum_{i=1}^{5} e_i$ and $y = 0$):

These sides of the panel apply Neumann conditions, which means that there is no heat flux across these boundaries.

- On Γ_{12}, Γ_{23}, Γ_{34}, and Γ_{45} (the interfaces between the layers):

According to the continuity of temperature and flux: for all $i, j \in \{1, 2, 3, 4, 5\}$, $i \neq j$

$$T_i = T_j \tag{2.12}$$

$$k_i \frac{\partial T_i}{\partial n} = k_j \frac{\partial T_j}{\partial n} \tag{2.13}$$

The continuity of temperature ($T_i = T_j$) ensures that there is no temperature jump at the interface between two adjacent layers. This is important because a discontinuity in temperature would be physically unrealistic and indicate an error in the heat transfer modeling.

The continuity of heat flux ($k_i \frac{\partial T_i}{\partial n} = k_j \frac{\partial T_j}{\partial n}$) ensures that the heat flux is conserved across the interface. In other words, the amount of heat leaving one layer must equal the amount of heat entering the adjacent layer. This condition is essential for maintaining thermal equilibrium in the system and accurately modeling the propagation of heat through the different layers of the photovoltaic panel.

3. Numerical solution

Solving the time-dependent heat transfer equation in a complex geometry, with several materials and heat sources, is a challenge. Typically, numerical methods such as the fully-explicit finite difference methods are used to solve such problems with domain decomposition.

3.1. Fully-explicit Finite Difference Methods

The fully-explicit finite difference method (FE-FDM) is a crucial numerical technique for solving partial differential equations (PDEs), such as the heat equation, over a two-dimensional domain. This approach relies on approximating spatial and temporal derivatives with finite differences, thus converting continuous differential equations into discrete algebraic systems that can be solved iteratively. The second-order spatial derivatives are approximated using central differences. For instance, the second-order derivative in the x-direction is approximated by

$$\frac{\partial^2 T}{\partial x^2} \approx \frac{T_{i+1,j} - 2T_{i,j} + T_{i-1,j}}{\Delta x^2}, \tag{3.1}$$

and in the y-direction by

$$\frac{\partial^2 T}{\partial y^2} \approx \frac{T_{i,j+1} - 2T_{i,j} + T_{i,j-1}}{\Delta y^2}. \tag{3.2}$$

The time derivative is approximated using a forward difference:

$$\frac{\partial T}{\partial t} \approx \frac{T_{i,j}^{n+1} - T_{i,j}^{n}}{\Delta t}. \tag{3.3}$$

By substituting these approximations into the heat equation, we obtain the discretized form:

$$\frac{\rho c \left(T_{i,j}^{n+1} - T_{i,j}^{n}\right)}{\Delta t} = k \left(\frac{T_{i+1,j}^{n} - 2T_{i,j}^{n} + T_{i-1,j}^{n}}{\Delta x^2} + \frac{T_{i,j+1}^{n} - 2T_{i,j}^{n} + T_{i,j-1}^{n}}{\Delta y^2} \right) + Q_{i,j}^{n}. \tag{3.4}$$

Rearranging this equation to isolate $T_{i,j}^{n+1}$, we obtain the explicit update formula:

$$T_{i,j}^{n+1} = T_{i,j}^{n} + \frac{k\Delta t}{\rho c} \left(\frac{T_{i+1,j}^{n} - 2T_{i,j}^{n} + T_{i-1,j}^{n}}{\Delta x^2} + \frac{T_{i,j+1}^{n} - 2T_{i,j}^{n} + T_{i,j-1}^{n}}{\Delta y^2} \right) + \frac{\Delta t}{\rho c} Q_{i,j}^{n}. \tag{3.5}$$

This formula calculates the temperature at time step $n+1$ based on the known values at time step n, the thermal properties of the material, and the internal heat generation. To ensure the stability of this explicit method, it is essential to carefully choose the time step Δt relative to the spatial steps Δx and Δy according to the Courant-Friedrichs-Lewy (CFL) stability criterion. The FE-FDM is particularly valued for its simplicity of implementation and computational efficiency in solving transient heat conduction problems on regular grids. This method is widely used to model thermal behaviors in complex systems, such as photovoltaic panels, thereby helping to identify hotspots and optimize thermal management to improve device performance and durability.

3.1.1. Statistical indices. To evaluate the quality and performance of our heat transfer model, we calculate several statistical indices defined in [8,9,11]. These indices provide quantitative measures of the model's accuracy and reliability under different environmental conditions.

- **Normalized Mean Squared Error (NMSE)**: The NMSE measures the average squared difference between observed (O) and modeled (M) values, normalized by the product of their means:

$$\text{NMSE} = \frac{\sum_{i=1}^{N} (T_{M_i} - T_{O_i})^2}{\sum_{i=1}^{N} T_{O_i} \cdot T_{M_i}} \tag{3.6}$$

- **Mean Relative Squared Error (MRSE)**: The MRSE is similar to NMSE but normalizes the squared differences by the square of the observed values:

$$\text{MRSE} = \frac{\sum_{i=1}^{N}\left(\frac{T_{M_i}-T_{O_i}}{T_{O_i}}\right)^2}{N} \tag{3.7}$$

- **Correlation Coefficient (COR)**: The COR assesses the linear relationship between observed and modeled values:

$$\text{COR} = \frac{\sum_{i=1}^{N}(T_{O_i} - \bar{T_O})(T_{M_i} - \bar{T_M})}{\sqrt{\sum_{i=1}^{N}(T_{O_i} - \bar{T_O})^2 \sum_{i=1}^{N}(T_{M_i} - \bar{T_M})^2}} \tag{3.8}$$

  where $\bar{O}$ and $\bar{M}$ are the means of observed and modeled values, respectively.

- **Fractional Bias (FB)**: The FB measures the average bias in the model predictions relative to the mean of the observed and modeled values:

$$\text{FB} = \frac{2\sum_{i=1}^{N}(T_{M_i} - T_{O_i})}{\sum_{i=1}^{N}(T_{M_i} + T_{O_i})} \tag{3.9}$$

- **Fractional Standard Deviation (FS)**: The FS compares the standard deviation of the observed and modeled values:

$$\text{FS} = \frac{\sigma_{T_M} - \sigma_{T_O}}{\bar{T_M} + \bar{T_O}} \tag{3.10}$$

  where σ_{T_M} and σ_{T_O} are the standard deviations of the modeled and observed values, respectively.

- **Geometric Mean Bias (MG):** It quantifies the multiplicative bias in model predictions, and is defined as:

$$\text{MG} = \exp\left(\frac{1}{N}\sum_{i=1}^{N}\ln\left(\frac{T_{M_i}}{T_{O_i}}\right)\right) \tag{3.11}$$

  Geometric Variance (VG): It represents the variance of the multiplicative bias and is defined as:

$$\text{VG} = \exp\left(\frac{1}{N}\sum_{i=1}^{N}\left(\ln\left(\frac{T_{M_i}}{T_{O_i}}\right) - \ln(\text{MG})\right)^2\right) \tag{3.12}$$

These statistical indices provide a comprehensive assessment of the model's performance. High COR values indicate strong linear correlations between observed and modeled temperatures. Low NMSE and MRSE values suggest minimal model errors, while FB and FS values near zero indicate low systematic bias and variability. MG and VG provide insight into the multiplicative bias and variance, respectively, further validating the model's accuracy and robustness.

3.2. Results presentation

This section is divided into two primary subsections: graphical temperature distributions and statistical indices. The graphical representations illustrate how varying levels of solar irradiance influence the thermal behavior of the PV panels, while the statistical comparisons provide a quantitative assessment of the model's accuracy and reliability.

The table 2 presents the absorptivity α for each layer of a typical polycrystalline silicon photovoltaic panel [14].

Layer	Absorptivity (α)
Glass	0.05
EVA	0.10
PV cells	0.90
Tedlar	0.05

Table 2: Absorptivity of Each Layer [14]

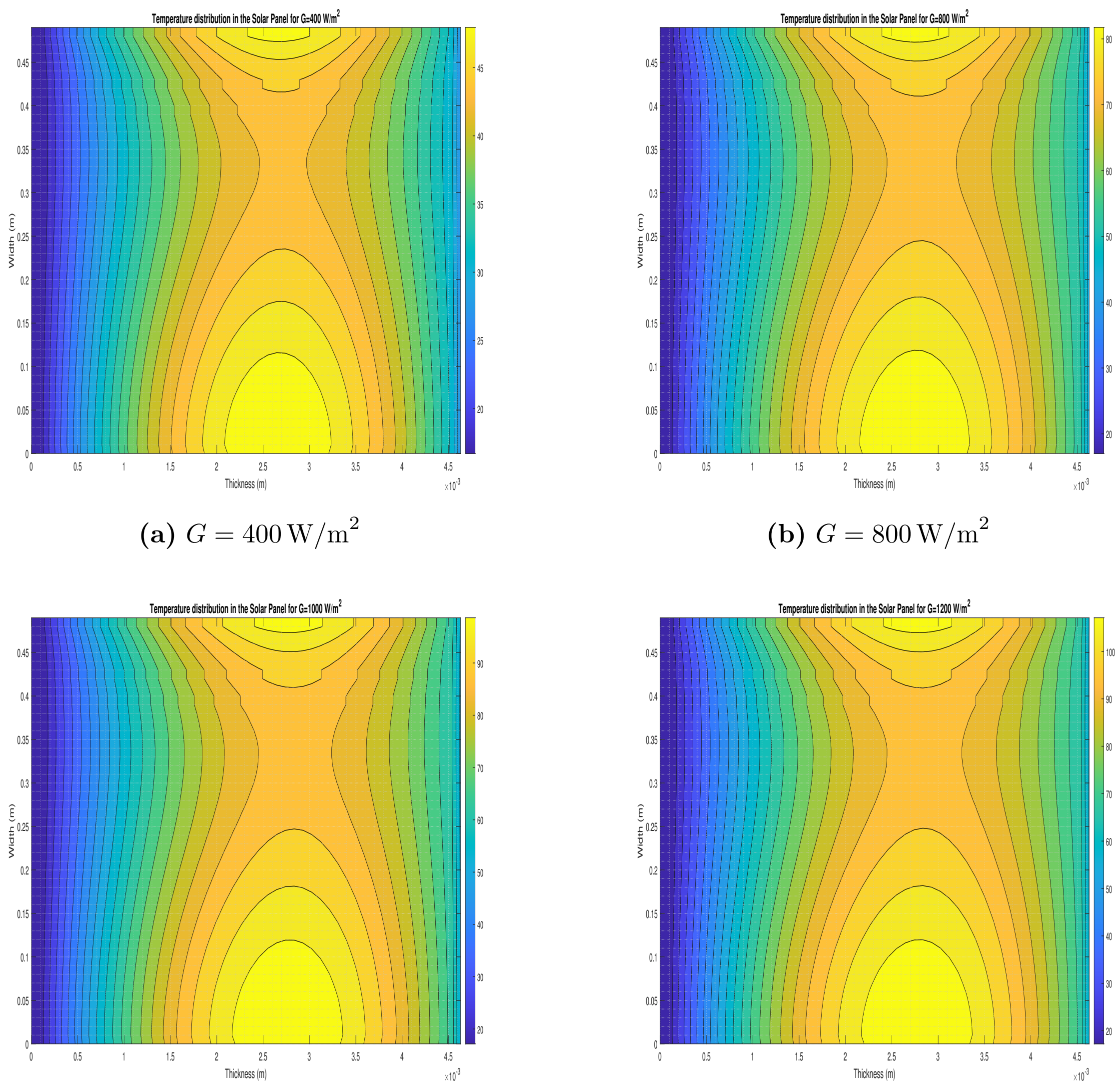

(a) $G = 400\,\mathrm{W/m^2}$

(b) $G = 800\,\mathrm{W/m^2}$

(c) $G = 1000\,\mathrm{W/m^2}$

(d) $G = 1200\,\mathrm{W/m^2}$

Figure 4: Temperature distributions in the solar panel for different irradiance values G, presented in 2D.

The temperature distribution clearly demonstrates the influence of solar irradiance on thermal behavior within the PV panel. As irradiance increases, heat accumulates predominantly in the PV cell layer due to its high absorptivity, leading to the emergence of thermal hotspots. The temperature gradient is oriented from the cell layer towards the external layers, with the Tedlar layer providing partial insulation at the rear. This behavior highlights the critical need for effective thermal management strategies to mitigate overheating and ensure consistent energy performance and panel longevity.

3.3. Model validation

To validate our model, we used daily experimental temperature data measured at the rear side of *ET-M53690WW* monocrystalline silicon PV panels installed at the renewable energy station of the National School of Applied Sciences (ENSA) in El Jadida, Morocco, where these panels are used for various practical applications.

3.3.1. Comparison between modeled and observed data. The comparison between observed and modeled temperature at the back of the PV panel on three days with different irradiances is presented in the following figure:

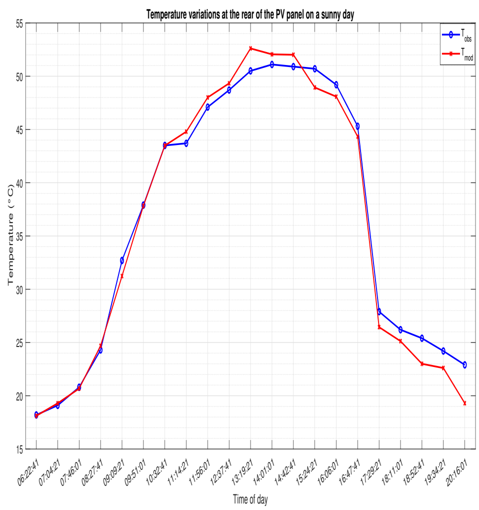

(a) Sunny day

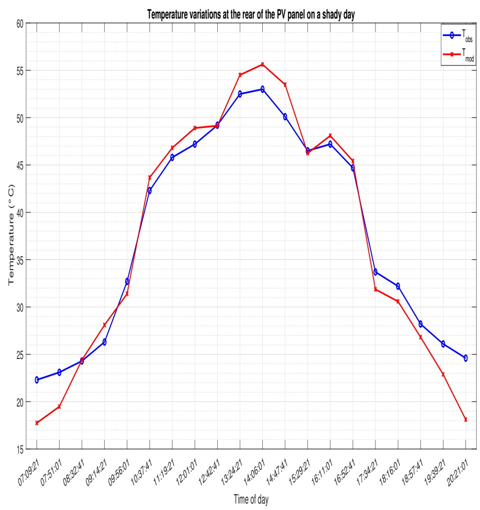

(b) Semi-shady day

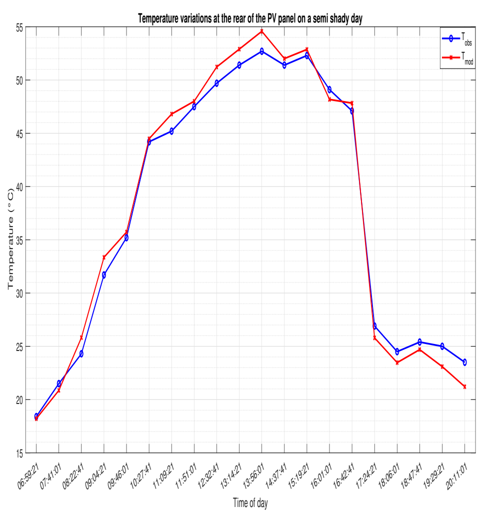

(c) Shady day

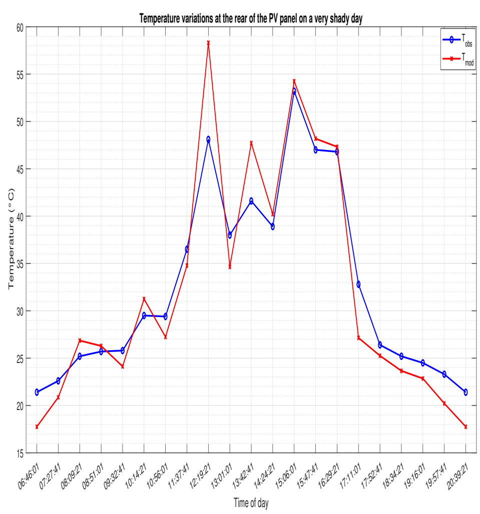

(d) Very shady day

Figure 5: Comparison between observed and modeled temperature under different sunlight conditions.

Table 3: Values of statistical indices for the heat transfer model for different days.

Statistical indices	Sunny day	Semi shady day (b)	Semi shady day (c)	Very shady day
NMSE	0.00151282	0.00459738	0.00108804	0.01142850
MRSE	0.00151278	0.00459722	0.00108804	0.01142823
COR	0.94819816	0.94234687	0.94724904	0.92532765
FB	-0.01099820	0.01161695	-0.00546800	0.00976203
FS	0.05279194	-0.16830344	-0.05869018	-0.20902751
MG	0.98075316	1.03535866	1.00225641	1.03311784
VG	1.00270760	1.01094216	1.00169823	1.01102321

4. Discussion

The findings of our study clearly indicate that thermal management is a critical factor in the operation and efficiency of photovoltaic panels. The ability to resolve the temperature distribution in two dimensions (thickness and width) has allowed the identification of potential overheating zones, which can significantly degrade cell performance. This detailed thermal insight opens up opportunities to optimize panel design by improving material selection and integrating more efficient heat dissipation strategies.

As shown in Figure 5 and supported by the statistical indices in Table 3, the comparison between simulated and experimentally measured temperatures at the rear surface (Tedlar layer) under different irradiance conditions (sunny, semi-shady, and very shady days) reveals a strong agreement. This concordance is particularly notable on clear days, confirming the model's capacity to capture the panel's thermal behavior accurately. Minor discrepancies under shaded conditions remain within acceptable margins, considering environmental variability. The consistently low error values (NMSE, MRSE) and high correlation coefficients (COR > 0.92) further reinforce the robustness and reliability of the proposed numerical model as a predictive and diagnostic tool for PV system thermal analysis.

5. Conclusion and Perspectives

This study emphasizes the critical importance of thermal management in improving the performance and durability of photovoltaic (PV) panels. Using a 2D fully explicit finite difference model, we accurately captured temperature gradients across both the thickness and width of multilayer PV structures. The model successfully integrates realistic boundary conditions and material properties, providing detailed thermal insights that are often neglected in simplified 1D or more computationally intensive 3D approaches.

Quantitatively, the model achieved strong agreement with experimental data, with correlation coefficients exceeding 0.94 and normalized mean square errors below 0.005 across various irradiance scenarios. These results validate the model's reliability and demonstrate its effectiveness for analyzing thermal behavior under realistic operating conditions. The identification of overheating zones further supports its application in guiding design choices for passive thermal regulation.

Nevertheless, the current model is limited to natural cooling conditions and assumes homogeneous material properties. Future developments will focus on incorporating active cooling strategies (e.g., misting or phase-change systems) and enabling real-time predictive thermal control, paving the way toward intelligent PV systems with enhanced adaptability to environmental fluctuations.

In summary, this work contributes both methodological and practical advancements to PV thermal modeling. It offers a robust and efficient tool for understanding and optimizing temperature distributions, with direct implications for the design and operation of next-generation solar energy systems.

Acknowledgements The authors would like to thank the referee warmly for his suggestions and valuable comments on this paper.

Include conflict of interest statement.

The authors declare that they have no conflicts of interest.

Data availability statement.
Not Applicable.
Author Contribution.
All authors are contributed equally in the paper.
Funding.
Not Applicable.

References

1. Ahliouati, M., El Otmani, R., & Kandoussi, K. (2023, May). Performance Analysis of Monocrystalline PV Module Under the Effect of Moroccan Arid Climatic Conditions. In 2023 3rd International Conference on Innovative Research in Applied Science, Engineering and Technology (IRASET) (pp. 1-6). IEEE.

2. Armstrong S., Hurley W.G., A thermal model for photovoltaic panels under varying atmospheric conditions, Appl. Therm. Eng. 30 (2010), 1488–1495.

3. Barroso, JC Sánchez, et al. "A computational analysis of coupled thermal and electrical behavior of PV panels." Solar Energy Materials and Solar Cells 148 (2016): 73-86.

4. Bergman, Theodore L. Fundamentals of heat and mass transfer. John Wiley & Sons, 2011.

5. Chouhan, Aditya, TYAGI, V. V., et ANAND, Sanjeev. Futuristic approach for thermal management in solar PV/thermal systems with possible applications. Energy conversion and management, (2018), vol. 163, p. 314-354.

6. El Achouby, H., M. Zaimi, A. Ibral, E.M. Assaid,: New analytical approach for modelling effects of temperature and irradiance on physical parameters of photovoltaic solar module, Energy conversion and management 177, (2018) 258-271.

7. ELAVARASAN, Rajvikram Madurai, MUDGAL, Vijay, SELVAMANOHAR, Leoponraj, et al. Pathways toward high-efficiency solar photovoltaic thermal management for electrical, thermal and combined generation applications: A critical review. Energy Conversion and Management, (2022), vol. 255, p. 115278.

8. Farhane, Mehdi, Omar Alehyane, and Otmane Souhar. "Three-dimensional analytical solution of the advection-diffusion equation for air pollution dispersion." The ANZIAM Journal 64.1 (2022): 40-53.

9. Hanna, S. R., D. G. Strimaitis, and J. C. Chang. "Hazard response modeling uncertainty (a quantitative method). Volume 1. User's Guide for Software for Evaluating Hazardous Gas Dispersion Models." Sigma Research Corporation, Westford (1991).

10. Hong, D., Ma, J., Wang, K., Man, K. L., Wen, H., & Wong, P. Real-Time Power Prediction for Bifacial PV Systems in Varied Shading Conditions: A Circuit-LSTM Approach Within a Digital Twin Framework. IEEE Journal of Photovoltaics, (2024), vol. 14, p. 652 - 660.

11. Kadyri A., Kandoussi K., Souhar O., An approach on mathematical modeling of PV module with sensitivity analysis: a case study. Journal of Computational Electronics, (2022), 1365-1372.

12. Khanna, V, Das, B., Bisht, D., Vandana and Singh, P.: "A three diode model for industrial solar cells and estimation of solar cell parameters using PSO algorithm," Renewable Energy, vol. 78, pp. 105-113 (2015)

13. Ko, J., Kim, K., Sohn, J. W., Jang, H., Lee, H. S., Kim, D., & Kang, Y. Review on Separation Processes of End-of-Life Silicon Photovoltaic Modules. Energies, 16(11), 4327 (2023).

14. Kudish, Avraham I., et al. "Simulation study of a solar collector with a selectively coated polymeric double walled absorber plate." Energy Conversion and Management 43.5 (2002): 651-671.

15. Lee Y., Tay A.A.O., Finite element thermal analysis of a solar photovoltaic module, Energy Procedia 15 (2012), 413–420.

16. Lewis, R. W., Nithiarasu, P., & Seetharamu, K. N. (2004). Fundamentals of the finite element method for heat and fluid flow. John Wiley & Sons.

17. Liu, J., and Shimoyama, K. Determination of Turbulent Prandtl Number for Thermal Fluid Dynamics Simulation of HVAC Unit by Data Assimilation. ASME. J. Thermal Sci. Eng. Appl, (2024), p. 1-10.

18. Naqvi, S.A.R., Kumar, L., Harijan, K., Sleiti, A.K.: "Performance investigation of solar photovoltaic panels using mist nozzles cooling system," *Energy Sources, Part A: Recovery, Utilization, and Environmental Effects*, vol. 46, no. 1, pp. 2299–2317 (2024). https://doi.org/10.1080/15567036.2024.2305302

19. Seyedmahmoudian, M., Mekhilef, S., Rahmani,R., Yusof, R. and Renani, E.T.: "Analytical Modeling of Partially Shaded Photovoltaic Systems," Energies, vol. 6, pp. 128-144 (2013)

20. Skoplaki E., Palyvos J.A., On the temperature dependence of photovoltaic module electrical performance: a review of efficiency/power correlations, Sol. Energy 83 (2009) 614–624,

21. Souhar, O. and Prud'homme, C.: "Numerical analysis method of heat transfer in an electronic component using sensitivity analysis," Journal of Computational Electronics, vol. 13, pp.1042-1053 (2014)

22. Swinbank W.C., Long-wave radiation from clear skies, Q. J. R. Meteorol. Soc. 89 (1963) 339–348

23. Tina G.M., Gagliano A., An improved multi-layer thermal model for photovoltaic modules, in: Proceedings of the Comput. Energy Sci. (SpliTech), Int. Multidiscip. Conf., IEEE, 2016, pp. 1–6.

24. Wilson, Edward L., and Robert E. Nickell. "Application of the finite element method to heat conduction analysis." Nuclear engineering and design 4.3 (1966): 276-286.

25. Yu, C., Shen, D., Tu, J., Chen, G., and Chai, L. Numerical analysis on thermal behavior of composite wall combined autoclaved aerated concrete with thermal insulting material in summer day. ASME. J. Thermal Sci. Eng. Appl, (2024), p. 1-12.

26. Zhou, J., Zhan, D., Qian, J., and Wei, T. Experimental investigation on the thermal performance of a large-size aluminum vapor chamber for multi-point heat sources. ASME. J. Thermal Sci. Eng. Appl, (2024), p. 1-19.

Abbes KADYRI,
Department of Mathematics,
Chouaib Doukkali University, El Jadida, 24000, Morocco.
E-mail address: kadyri.a@ucd.ac.ma

and

EL MAHDI ASSAID,
Department of Physics,
Chouaib Doukkali University, El Jadida, 24000, Morocco.
E-mail address: assaid.e@ucd.ac.ma

and

Khalid KANDOUSSI,
National School of Applied Sciences,
Chouaib Doukkali University, El Jadida, 24000, Morocco.
E-mail address: kandoussi.k@ucd.ac.ma

and

Otmane SOUHAR,
Department of Mathematics,
Chouaib Doukkali University, El Jadida, 24000, Morocco.
E-mail address: souhar.o@ucd.ac.ma